ELSEVIER

Journal of Crystal Growth 151 (1995) 21-25

JOURNAL OF CRYSTAL GROWTH

Metalorganic chemical vapor deposition of $Ga_xIn_{1-x}Sb$ ternary alloys

Zhang Baolin *, Zhou Tianming, Jiang Hong, Ning Yongqiang, Jin Yixin, Hong Chunrong, Yuan Jinshan

Changchun Institute of Physics, Chinese Academy of Sciences, 130021 Changchun, People's Republic of China

Received 9 August 1994; manuscript received in final form 24 January 1995

Abstract

Metalorganic chemical vapor deposition (MOCVD) of ternary $Ga_xIn_{1-x}Sb$ alloys on GaSb and GaAs substrates has been investigated at atmospheric pressure, using TMGa, TMIn and TMSb as source materials. The optimized growth parameters obtained by experiment were a growth temperature of 600°C and a vapor III/V ratio of 0.4. It was found that the growth temperature was a key growth parameter for surface morphology and crystalline quality of the $Ga_xIn_{1-x}Sb$ epilayer. The influence of the growth temperature on the Ga solid composition was previously explained. The Ga solid composition was proportional to the Ga vapor composition and vapor III/V ratio, respectively. The Ga distribution coefficient was found to be 1.06 under the optimized growth parameters and decreased with decreasing growth temperature. The results of the Hall measurement for $Ga_xIn_{1-x}Sb$ alloys were presented with p-type background of the epilayers.

1. Introduction

Sb-containing III–V compounds are potentially semiconductor materials for the infrared technology. These materials can be used to fabricate a number of useful narrow bandgap devices, such as lasers [1,2] and detectors [3–5]. $Ga_xIn_{1-x}Sb$, $InAs_{1-y}Sb_y$ ternary alloys and $Ga_xIn_{1-x}As_{1-y}Sb_y$, $InAs_{1-x-y}P_xSb_y$ quaternary alloys are the narrow bandgap semiconductors whose direct energy bandgaps correspond to wavelengths over a wide spectral range from 0.87 to 12 μm. They are applied in infrared research, IR focal plane arrays (FPA), space technology and optical fiber communications in the 2–4 μm range.

The energy bandgap of $Ga_xIn_{1-x}Sb$ ternary alloys varies from 0.175 to 0.67 eV with the solid composition (Ga-content in alloys), x, ranging from 0 to 1, corresponding to the wavelength range 7–1.85 μm.

MOCVD growth of $Ga_xIn_{1-x}Sb$/GaSb [6–11] and characterization of p–n photodiodes [7] and quantum-well structure [11] have been studied. Fashe et al. [12] and Chow et al. [13] have reported successful molecular beam epitaxy (MBE) growth of $Ga_xIn_{1-x}Sb$/InAs superlattices, which have been proposed for far-infrared applications [14,15]. Kaneko et al. [16] have reported, for the first time, metalorganic molecular beam epitaxy (MOMBE) growth of GaInSb alloys on GaSb substrates.

In this paper, we report the MOCVD growth results of unintentionally doped $Ga_xIn_{1-x}Sb$ epilayers. In particular, the influence of growth parameters upon the Ga solid composition in $Ga_xIn_{1-x}Sb$ alloys has been studied in detail.

* Corresponding author.

SSDI 0022-0248(94)01022-6

Table 1
Growth parameters of $Ga_xIn_{1-x}Sb$ ternary alloys

Growth temperature	(°C)	560–640
TMGa source temp.	(°C)	−12
TMIn source temp.	(°C)	15
TMSb source temp.	(°C)	0
TMGa flow rate	(mol/min)	$(5–10)\times10^{-6}$
TMIn flow rate	(mol/min)	$(1.3–6.5)\times10^{-6}$
TMSb flow rate	(mol/min)	$(20–30)\times10^{-6}$
Vapor III/V ratio		0.2–1.5
Ga vapor composition		0.4–0.9
Total H_2 flux	(l/min)	2.5–4

2. Experimental procedure

Ternary $Ga_xIn_{1-x}Sb$ alloys were grown by MOCVD in a horizontal, RF-heated reactor at atmospheric pressure. Trimethylgallium (TMGa), trimethylindium (TMIn) and trimethylantimony (TMSb) were used as Ga, In and Sb sources, respectively. All of them are the products of Dalian Guangming Research Institute of Chemical Industry of China. TMGa, TMIn and TMSb were held in coolers at temperatures of −12, 15 and 0°C, respectively. Palladium-diffused pure hydrogen was used as carrier gas in this experiment.

The substrates used were Te doped n-type GaSb wafers with a net donor concentration of 5×10^{17} cm^{-3} and Cr doped semi-insulating GaAs wafers, both with an orientation 2° off (100) towards ⟨110⟩. They were treated with conventional chemical methods. GaSb substrates were etched by a mixed solution of nitric acid, hydrochloric acid, and ice-acetic acid ($HNO_3 : HCl : CH_3COOH$= 0.2 : 2 : 10), while GaAs substrates were prepared by a standard chemical etching solution ($H_2SO_4 : H_2O : H_2O_2 = 5 : 1 : 1$).

The GaSb substrate was protected by the TMSb gas flow from decomposition of GaSb before growth, and for the same reason, the $Ga_xIn_{1-x}Sb$ epilayer was also protected by TMSb flows at the end of growth.

Typical growth parameters used in the experiment are given in Table 1.

$Ga_xIn_{1-x}Sb$ surface morphology was observed by means of optical microscopy and scanning electron microscopy (SEM). Solid compositions of the $Ga_xIn_{1-x}Sb$ epilayers were determined by X-ray diffraction and electron microprobe analysis, respectively. X-ray diffraction was also used to determine

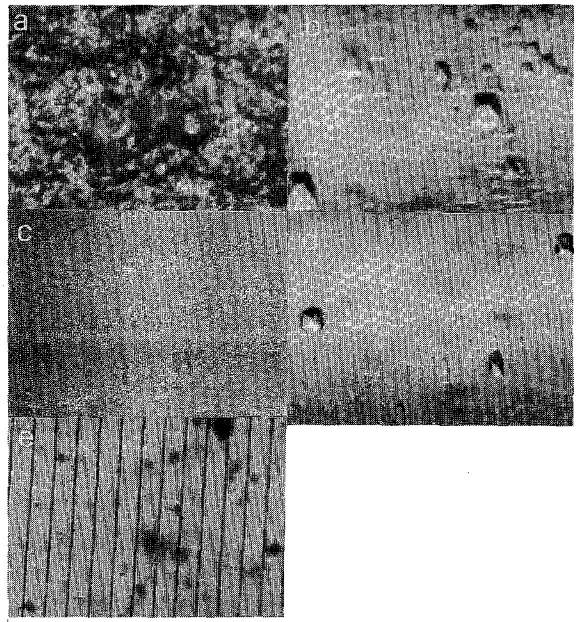

Fig. 1. Surface morphologies of $Ga_xIn_{1-x}Sb$ layers on GaSb substrates for different growth temperatures, III/V = 0.4 and $x^v = 0.7$. (a) T_g = 560°C, x = 0.22; (b) T_g = 580°C, x = 0.65; (c) T_g = 600°C, x = 0.75; (d) T_g = 620°C, x = 0.78; (e) Marking lines, 1 μm adjacent lines.

the epilayers' crystalline quality. A standard Van der Pauw–Hall measurement was employed to evaluate the electric properties of $Ga_xIn_{1-x}Sb$ layers deposited on SI-GaAs substrates.

3. Results and discussion

The $Ga_xIn_{1-x}Sb$ surface morphologies were observed by SEM. Surface defects with pyramids in $Ga_xIn_{1-x}Sb$ epilayers are generated more easily than

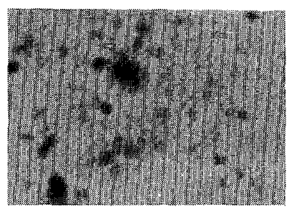

Fig. 2. $Ga_xIn_{1-x}Sb$ surface morphology with cross grid of misfit dislocations. T_g = 600°C, III/V = 0.5, x^v = 0.5.

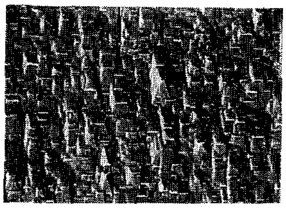

Fig. 3. Surface morphology of $Ga_xIn_{1-x}Sb$ layer on GaAs substrate, $T_g = 600°C$, III/V = 0.4, $x^v = 0.7$.

in other III–V ternary alloys during growth because antimony has a negligible vapor pressure comparing with arsenic and phosphorus at growth temperature. However, a nearly mirror-like surface was obtained under the optimized growth parameters with a growth temperature of 600°C, III/V = 0.4 and x^v = 0.7. Fig. 1 shows the surface morphologies of the epilayers at different growth temperatures (560, 580, 600 and 620°C, respectively) with III/V = 0.4 and x^v = 0.7. 560°C growth always leads to a poor surface morphology with Sb metallic droplets. At 580°C, surface defects with pyramids appear. Increasing the growth temperature results in a pyramid's density decrease. Then, when the temperature was beyond 620°C, the density starts to increase. At a higher growth temperature, InSb droplets were formed due to the lower melting point of the InSb component. The typical surface morphology with a cross grid of misfit dislocations, as seen from Fig. 2, illustrates that the lattice constant of the mismatched grown $Ga_xIn_{1-x}Sb$ layer is larger than that of the GaSb substrate. In contrast, $Ga_xIn_{1-x}Sb$ suface morphologies on GaAs substrates have different textures (Fig. 3), which may be caused by lattice relaxation due to the large lattice mismatch ($\Delta a/a = 8\%$).

Surface morphologies of $Ga_xIn_{1-x}Sb$ epilayers with different Ga solid compositions were observed. Smooth mirror-like surfaces were always obtained when x greater than 0.8 under proper growth parameters, where the lattice mismatches are less than 1.1×10^{-2}. Decreasing x, the surface morphology deteriorates gradually and some pyramids or an irregular mosaic structure appear since the lattice mismatch between the $Ga_xIn_{1-x}Sb$ epilayer and the GaSb substrate increases with x decreasing.

The X-ray diffraction patterns for four $Ga_xIn_{1-x}Sb$ samples deposited on GaSb substrates under different

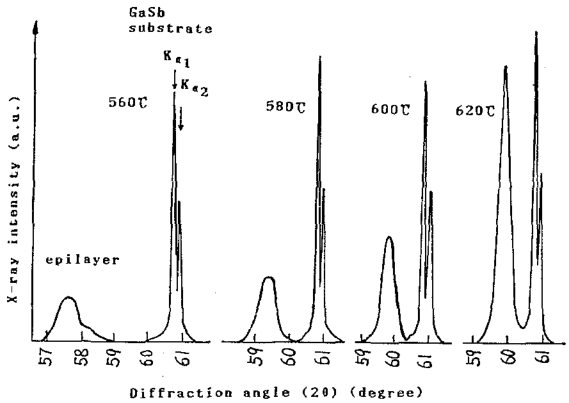

Fig. 4. X-ray diffraction patterns for four $Ga_xIn_{1-x}Sb$/GaSb samples under different growth temperatures, III/V = 0.4, x^v = 0.7.

growth temperatures at the same III/V ratio of 0.4 and x^v of 0.7, are shown in Fig. 4. (Relevant Ga solid compositions are 0.22, 0.65, 0.75 and 0.78, respectively, as shown in Fig. 5.) Fig. 4 illustrates that the epilayers' crystalline quality degrades with decreasing growth temperature due to the lattice mismatch increases, corresponding to the result of the study for surface morphology.

It can be seen from Fig. 5 that the Ga solid com-

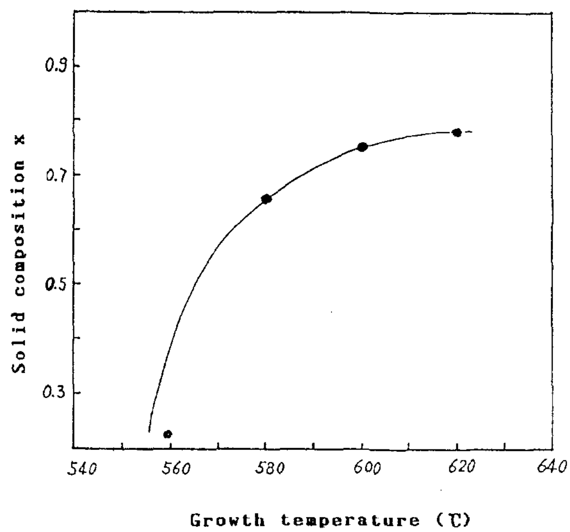

Fig. 5. Solid composition of $Ga_xIn_{1-x}Sb$ alloys versus growth temperature, III/V = 0.4, x^v = 0.7.

position x increases rapidly with increasing growth temperature from 560 to near 600°C, and then x increases very slowly as the growth temperature is up to 620°C. There are two explanations for the variation. It is known that the pyrolysis temperature of TMGa is higher than that of TMIn, which pyrolyses completely at 500°C [17]. In the range 560–600°C, the TMGa pyrolysis efficiency increases rapidly with increasing growth temperature. Then, above 600°C, TMGa is nearly completely pyrolysed. Accordingly, the curve of the Ga solid compositions becomes horizontal at higher temperature, but there is little agreement in the literature on the subject of TMGa pyrolysis. Nishizawa and Kurabayashi [18] report the fraction pyrolysed at 500°C to be only 0.17. Yoshida et al. [19] report complete pyrolysis of TMGa at 460°C. Another explanation was made by Bougnot and coworkers [6,7] and Su et al. [9]: The GaSb growth rate is thermally activated between 530 and 600°C whereas the InSb growth rate seems to be constant in the same range. So, the GaSb solid mole fraction increased and the InSb solid mole fraction decreased with increasing temperature.

The Ga vapor composition x^v (TMGa mole fraction in the reactor, $x^v = F_{TMGa}/(F_{TMGa} + F_{TMIn})$) has an important effect on the Ga solid composition x. The dependence of x on x^v is shown in Fig. 6. The III/V ratio was taken as 0.4 and the growth temperature was 600 and 580°C, respectively. It is clearly seen that the solid composition x is in direct proportion to the vapor composition x^v. The Ga distribution coefficients K_{Ga} ($K_{Ga} = x/x^v$) are near unity, 0.91 at 580°C and 1.06 at 600°C . It is in good agreement with the result reported by Bougnot et al. [6] ((o) as seen in Fig. 6) and is consistent with the results reported by Yuan et al. [20] for MOVPE $Ga_yIn_{1-y}P$ and Stringfellow [21] for GaInAs. The Ga distribution coefficient decreased with reduced growth temperature, which is, in fact, the same result as that shown in Fig. 4. So, this variation is also explained by the discussion above for the variation of the Ga solid composition with growth temperature. The influence of the vapor III/V ratio ($(F_{TMGa} + F_{TMIn})/F_{TMSb}$) in the reactor upon the Ga solid composition was studied at T_g = 600°C and x^v = 0.8. As shown in Fig. 7, the solid composition x is also in proportion with the vapor III/V ratio.

It has been found by experiment that the Ga distribution coefficient of the $Ga_xIn_{1-x}Sb$ epilayer on the GaSb substrate is less than that on the GaAs substrate.

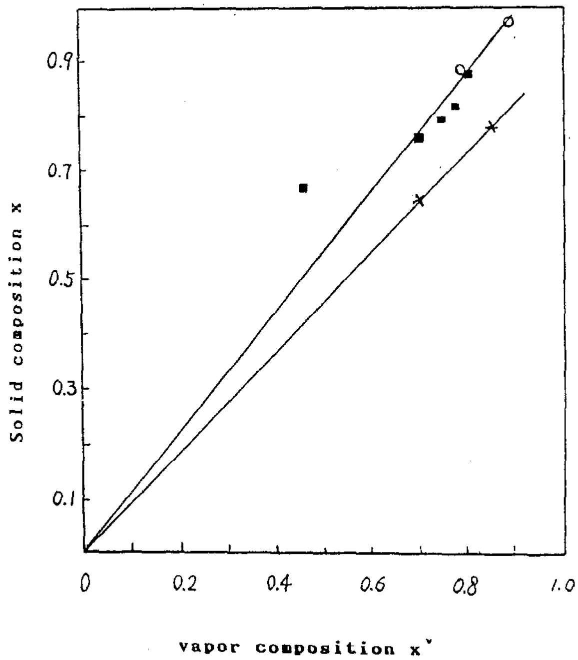

Fig. 6. Variation of $Ga_xIn_{1-x}Sb$ solid composition versus vapor composition under different temperatures, III/V = 0.4. (■) Our results, 600°C, k_{Ga} = 1.06; (×) Our results, 580°C, k_{Ga} = 0.91; (o) Bougnot et al. [6], 600°C.

The electrical properties of $Ga_xIn_{1-x}Sb$ alloys deposited on SI-GaAs substrates were measured using the Van der Pauw technique. The Hall measurement results are listed in Table 2. Unintentionally doped layers are of p-type and the higher hole mobility is as large as 377 $cm^2/V\cdot s$ (x = 0.82), corresponding to a hole concentration of 5×10^{16} cm^{-3}. The data

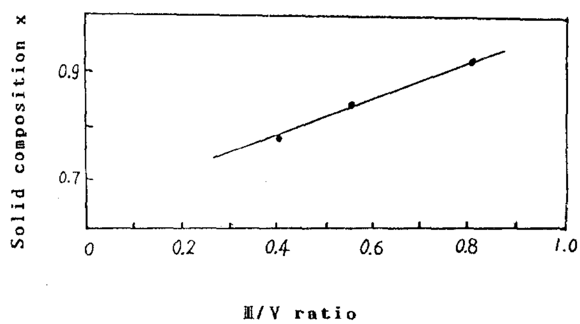

Fig. 7. Influence of vapor III/V ratio in reactor upon the Ga solid composition x of $Ga_xIn_{1-x}Sb$ alloys, T_g = 600°C, x^v = 0.7.

Table 2
Hall measurement results of $Ga_xIn_{1-x}Sb$ epilayers

Sample No.	x	μ ($cm^2/V \cdot s$)	p (cm^{-3})
1111	0.76	339	1.7×10^{17}
1113A	0.82	377	7.6×10^{16}
1113B	0.87	222	1.0×10^{17}

are comparable to the best electrical results reported to date for $Ga_xIn_{1-x}Sb$ alloys [7,10].

4. Conclusion

The ternary $Ga_xIn_{1-x}Sb$ alloys were grown on n-type GaSb and SI-GaAs substrates using the MOCVD technique at atmospheric pressure. It has been found that the growth temperature is a key growth parameter for the surface morphology and crystalline quality of the $Ga_xIn_{1-x}Sb$ epilayer and the optimized growth temperature is fixed to 600°C. The characteristic results demonstrate the Ga solid compositions of $Ga_xIn_{1-x}Sb$ alloys were dependent on the growth temperature and were in proportion to the Ga vapor composition and the vapor III/V ratio, respectively. The Ga distribution coefficients of the epilayers on GaSb substrates decreased as decreasing the growth temperature and present smaller values comparing with those on GaAs substrates. Unintentionally doped $Ga_xIn_{1-x}Sb$ layers always give p-type conduction and the higher mobility reaches to 377 $cm^2/V \cdot s$.

Acknowledgements

The authors would like to thank Mr. Liu Naikang and Mrs. Jiang Jinxiu for scanning electron microscopy and electron microprobe analysis and Mr. Ge Zhongjiu for the X-ray measurement. This work is supported by the National Advanced Material Committee of China under grant 863-715-01-03-01.

References

[1] C. Caneau, A.K. Sriyastava, A.G. Dentai, J.L. Zyskind and M.A. Pollack, Electron. Lett. 21 (1985)815.
[2] S.J. Eglash, H.K. Choi and G.W. Turner, J. Crystal Growth 111 (1991) 669.
[3] C. Hilsum and H.D. Rees, Electron. Lett. 6 (1970) 277.
[4] J.E. Bowers, A.K. Srivastava, C.A. Burrus, J.C. DeWinter, M.A. Pollack and J.L. Zyskind, Electron. Lett. 22 (1986) 137.
[5] J.L. Zyskind, C.A. Burrus, C. Caneau, A.G. Dentai, M.A. Pollack and A.K. Srivastava, Components for Fiber Optic Applications, SPIE 722 (1986) 200.
[6] G.J. Bougnot, A.F. Foucaran, M. Marjan, D. Etienne, J. Bougnot, F.M.H. Delannoy and F.M. Roumanille, J. Crystal Growth 77 (1986) 400.
[7] G. Bougnot, F. Delannoy, A. Foucaran, F. Pascal, F. Roumaiille, P. Grosse and J. Bougnot, J. Electrochem. Soc. 135 (1988) 1783.
[8] E.T.R. Chidley, S.K. Haywood, R.E. Mallard, N.J. Mason, R.J. Nicholas, P.J. Walker and R.J. Warburton, J. Crystal Growth 93 (1988) 70.
[9] Y.K. Su, F.S. Juang and T.S. Wu, J. Appl. Phys. 70 (1991) 1421.
[10] G. Bougnot, F. Delannoy, F. Pascal, P. Grosse, A. Giani, J. Kaoukab, J. Bougnot, R. Fourcade, P.J. Walker and N.J. Mason, J. Crystal Growth 107 (1991) 502.
[11] S.K. Haywood, E.T.R. Chidley, R.E. Mallard, A.J. Mason, R.J. Nicholas, P.J. Walker and R.J. Warburton, Appl. Phys. Lett. 54 (1989) 922.
[12] R. Fashe, J.T. Zborowski, T.D. Golding, H.D. Shin, P.C. Chow, K. Matsuichi, B.C. Covington, A. Chi and J. Zheng, J. Crystal Growth 111 (1991) 677.
[13] D.H. Chow, R.H. Miles and C.W. Nieh, J. Crystal Growth 111 (1991) 683.
[14] C. Mailhiot and D.L. Smith, J. Vac. Sci. Technol. B 5 (1987) 1268.
[15] C. Mailhiot and D.L. Smith, J. Vac. Sci. Technol. A 7 (1989) 445.
[16] T. Kaneko, H. Aashi, Y. Okuno and S. Gonda, J. Crystal Growth 95 (1989) 158.
[17] C.A. Larsen and G.B. Stringfellow, J. Crystal Growth 75 (1986) 247.
[18] J. Nishizawa and T. Kurabayashi, J. Electrochem. Soc. 130 (1983) 413.
[19] M. Yoshida, H. Watanabe and F. Uesugi, J. Electrochem. Soc. 132 (1985) 677.
[20] J.S. Yuan, C.H. Chen, R.M. Cohen and G.B. Stringfellow, J. Crystal Growth 78 (1986) 63.
[21] G.B. Stringfellow, J. Crystal Growth 68 (1984) 111.